

to future vehicles that require high levels of performance and reliability.

References

¹ Kendrick, J. B. and Imus, R. E., "The pumping of liquid rocket propellant by injecting fuel into oxidizer tank," Jet Propulsion Lab. Rept. 4-19, California Institute of Technology, Pasadena, Calif. (May 1948); also Tapp, J., "Chemical and other means of propellant-tank pressurization," Final Report, R-470, Contract AF33(038)-2733, Aerojet Engineering Corp., Azusa, Calif. (September 1950).

² Zeleznick, F. J. and Gordon, S., "A general IBM7090 computer program for computation of chemical equilibrium compositions, rocket performance, and Chapman-Jouget detonations," NASA TN-D-1454 (1962), and Suppl. I, NASA TN-D-1737 (1963).

Bibliography

Kenny, R. J., Friedman, P. A., Lane, A. P., and Bingham, P. E., "Development and demonstration of main tank injection (MTI) pressurization system," Final Rept. RTD-TDR-63-1123, Martin Co., Denver Div., Denver, Colo. (December 1963).

Binkhoff, G. and Zarentovelle, E., *Jets, Wakes and Cavities* (Academic Press Inc., New York, 1957).

Morey, T. F., "N₂O₄ thermodynamic properties," TM 0431-302, Martin Co. (October 1960).

Sutton J. F., et al., "Main propellant tank pressurization system study and test program," SSD-TR-61-21, Vol. III, Design Handbook, Lockheed Aircraft Corp., Marietta, Ga. (December 1961).

Heaton, T. R. and Roberts, F. L., "In-tank reaction for propellant pressurization," Supplement to Bulletin of Fourth Liquid Propellant Joint Army-Navy-Air Force-NASA-ARPA Symposium, CPIA Publication No. 8 (February 1963) (Confidential).

Allen, C. H., "In-tank reaction for propellant pressurization," Fifth Liquid Propellant Information Agency Symposium, Paper L-62-383R (1962).

Ignition and Combustion of Aluminum in Small-Scale Liquid Rocket Engines

L. E. DEAN,* R. C. KEITH,† T. L. SUMNER,‡ AND M. V. TAYLOR§
Aerojet-General Corporation, Sacramento, Calif.

The combustion of aluminum particles was investigated in nine O₂(gas)-H₂(gas)-Al burner tests and 20 100-lbf-thrust O₂(gas)-H₂(gas)-Al rocket-engine tests. The aluminum powder was transported to the burner or the thrust chamber by entraining it in the H₂ gas by means of a pneumatic transport system. The burner tests indicated that the ignition delay of aluminum powder clouds was dependent on the O₂-H₂ flame temperature and on the aluminum particle concentration. The 100-lbf-thrust engine tests, conducted at a nominal chamber pressure of 300 psia, yielded an experimental specific impulse of approximately 80% of the theoretical value. The major areas of performance loss, in terms of percent of theoretical specific impulse, were heat transfer and deposition, 10%; nozzle geometry and shear drag, 3%; and gas-particle flow losses, 1%. The corrected experimental *I_s* is about 94% of the theoretical specific impulse.

Introduction

THEORETICAL calculations have indicated that the performance of many propellant systems can be increased by metal additives. Maximum specific impulse usually occurs when the metal additive is burned stoichiometrically, and the hydrogen is utilized as a working fluid. The metal to be used as an additive should have a low molecular weight and a high heat of combustion. The O-H-Al system was chosen for the experimental work. Gaseous oxygen and hydrogen were used to minimize operational difficulties, and the aluminum was delivered to the combustor in the form of powder suspended in the H₂ gas.

Metal powder combustion was reviewed by Hartmann¹ and more recently by Markstein.² Friedman and Macek³ found

Presented at the AIAA Heterogeneous Combustion Conference, Palm Beach, Fla., December 11-13, 1963 (not preprinted); revision received February 25, 1965.

* Manager, Engineering Research Department, Research and Advanced Technology Division, Liquid Rocket Plant. Member AIAA.

† Manager, Physics Laboratory, Research and Advanced Technology Division, Liquid Rocket Plant.

‡ Project Engineer, Engineering Research Department, Research and Advanced Technology Division, Liquid Rocket Plant.

§ Chemist, Engineering Research Department, Research and Advanced Technology Division, Liquid Rocket Plant.

that, when single particles of aluminum were injected into a propane-air flame, ignition took place only when the flame temperature was above 4100°R. Since the respective melting points of aluminum and aluminum oxide are 1678° and 4172°R [Joint Army-Navy-Air Force (JANAF) data], the high ignition temperature of the aluminum was attributed to the protective effect of the inert oxide coating present on the metal particle. The coating isolated the unreacted metal from the oxidizing atmosphere, thus ignition could occur only when the oxide coating melted and allowed the oxygen to diffuse through the molten oxide and react with the metal and/or the metal to diffuse through the oxide shell to react with the oxygen atmosphere.

The earlier work of Gordon⁴ also demonstrated that a temperature greater than 4200°R was required to ignite single aluminum particles. Gordon also determined that a cloud of aluminum particles would ignite and burn at a much lower flame temperature than an isolated aluminum particle. Gordon attributed the decrease in ignition temperature to the cooperative effects of the many particles heating the surrounding medium and to the conservation of radiant energy by reabsorption by neighboring particles. The same "cloud" effect was also found to occur in the ignition of boron.

Cassel and Liebman⁵ found that the ignition temperature of magnesium and 50-50 magnesium-aluminum alloys decreased as the dust concentration increased. They pointed

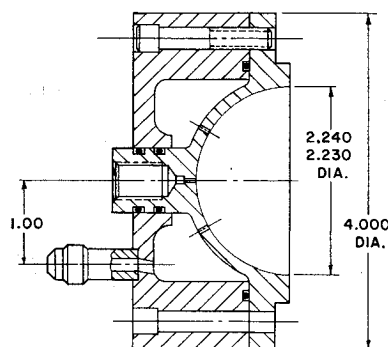


Fig. 1 Hemispherical stainless-steel injector.

out that the decrease in ignition temperature with increasing particle concentration was due to the reduced distance between particles and to the increase in the total heat-generating area. Cassel and Liebman observed that, with small concentrations, particle ignition was not achieved uniformly throughout the cloud but rather originated in sporadically distributed centers in flamelets, which then engulfed the whole cloud.

Experimental Equipment

Burner

The initial experiments to study the ignition and combustion characteristics of aluminum powder were performed with a Victor premix oxygen-hydrogen welding torch. The oxygen gas is injected into the premix portion of the torch through a swirler, where the hydrogen gas and aluminum powder mix with the oxygen. The $\frac{5}{8}$ -in.-diam copper burner tip has one hole in the center with 12 holes symmetrically rimming the tip. The holes are 0.062 in. in diameter. The aluminum powder is transported by the pneumatic transport system as described below. The ignition and combustion of the aluminum powder were recorded with a Fastax camera on Kodachrome-II color film at F numbers of 4 and 5.6 at 1000 frames/sec.

Rocket Engine

The hemispherical, stainless-steel injector (Fig. 1) used for the performance tests has four streams of oxygen gas impinging on a central fuel stream, which contains all of the aluminum-powder flow and 10% of the total hydrogen-gas flow. Impingement of the propellant streams was 1.125 in. from the injector face (center of radius).

The remaining 90% of the hydrogen gas was injected into the chamber by a stainless-steel ring placed between chamber segments or between the injector and the first chamber segment (Fig. 2). The hydrogen was injected through six orifices in the ring with an included angle of impingement of 60° or 120°.

In order to conveniently vary L^* and the hydrogen ring placement during the tests, the copper combustion chamber was made of segments with an inside diameter of 2.25 in. and an L^* , i.e. (chamber volume)/(throat area), of 50. The copper nozzles had a 0.531-in. throat diameter and an ex-

pansion ratio of 3.5. The nozzle converging section added 20 in. to the L^* of the chamber.

Propellant Feed System

Hydrogen and oxygen were supplied from standard high-pressure gas cylinders and the flow rates measured with critical flow orifices with known calibration factors. The aluminum powder was delivered to the combustion chamber by entrainment in approximately 10% of the total hydrogen flow. A schematic diagram of the powder feed system is shown in Fig. 3.

Since the powder flow rate was found to be proportional to the gas velocity, the carrier H_2 flow rate was regulated with critical flow orifices. The average aluminum-powder flow rate was determined by weighing the powder reservoir before and after each test.

Preliminary Ignition and Combustion Tests

Burner Tests

Six O_2 - H_2 -Al burner tests were made using Reynolds 400 aluminum powder in which approximately 98% of the aluminum particles were determined by optical microscopy to have diameters not exceeding 5 μ . The test conditions are given in Table 1. The hydrogen flow rate was 0.00175 lb/sec, and the oxygen flow rate was either 0.00262 or 0.00875 lb/sec, corresponding to O_2 - H_2 mass mixture ratios (MR) of 1.5 or 5.0. The O_2 - H_2 flame stabilized on the burner tip and was about 0.25 in. high. The burner was not shrouded, so the O_2 - H_2 combustion products were mixed with secondary air.

Analysis of the photo coverage of the burner tests indicated that the aluminum particles were preheated as they were carried through the O_2 - H_2 flame and then burned with the O_2 - H_2 combustion products. Tests B-1, B-2, and B-3, conducted at $MR = 1.5$, demonstrated an appreciable preheat zone where the aluminum particles were heated to a red glow before they burned with a brilliant white flame. In test B-1, conducted with an aluminum-powder flow rate of 0.00157 lb/sec, the preheat zone was about 3 in. long. In test B-2, with an aluminum powder flow rate of 0.0070 lb/sec, and test B-3, with an aluminum powder flow rate of 0.0304 lb/sec, the preheat zone was about 1 in. long. The aluminum particles burned at an ignition temperature (3050°R) far below the melting point of the oxide (4172°R). This lowering of the ignition temperature due to cloud effects was consistent with the work done by Gordon⁴ and that done by Cassel and Liebman.⁵ It was also observed that, during the tailoff of the powder injection, as the concentration of the aluminum powder diminished, the aluminum (at the unknown flow rate) stopped burning and appeared as a red glow.

Table 1 Burner test summary

Test no.	O_2 - H_2 MR	O_2 - H_2 flame temperature, °R	Al powder ^a flow rate, lb/sec
B-1	1.5	3050	0.00157
B-2	1.5	3050	0.0070
B-3	1.5	3050	0.0304
B-4	5	5400	0.1385
B-5	5	5400	0.0321
B-6	H_2 only	...	0.0344
B-7 ^b	1.5	3050	0.0750
B-8 ^b	5	5400	0.0633
B-9 ^b	1.5	3050	0.0428

^a Aluminum powder used was Reynolds 400 with an average particle size of 5 μ .

^b Baker USP aluminum powder, average particle size of 44 μ .

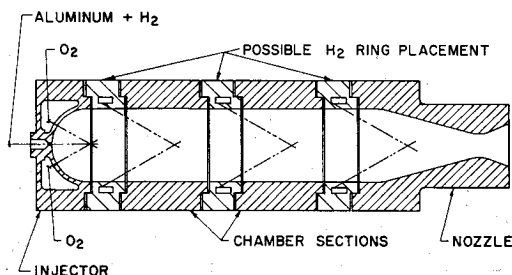


Fig. 2 Rocket-engine schematic diagram.

Tests *B-4* and *B-5*, conducted at $MR = 5$, produced a considerably shorter preheat zone with the aluminum particles burning slightly above the burner tip. This indicates that an increase in the O_2 - H_2 flame temperature (to $5400^\circ R$) decreases the ignition time of the aluminum powder. However, any direct correlation of temperature with ignition delay is difficult because of the varying amounts of oxygen available for the aluminum combustion. Available oxygen is dependent on the MR and the secondary air entrainment.

To determine the effect of secondary air entrainment, test *B-6* was made using only hydrogen gas and aluminum powder. In this test, hydrogen burned with the air, and the brilliant white flame indicative of the aluminum ignition appeared at approximately the same distance from the burner tip as in the flame resulting from an O_2 - H_2 MR of 1.5. It appears that at the lower MR 's the aluminum burned primarily with the entrained secondary air, whereas at the higher MR 's some combustion was due to the higher oxygen content of the flame.

Three burner tests were made using coarser aluminum powder [Baker United States Pharmacopoeia (USP) grade] with an average particle size of $44\ \mu$. Two tests were made using an O_2 - H_2 MR of 1.5 and one at an MR of 5 (Table 1). The results of the former two tests were similar to the results of the tests using $5\text{-}\mu$ aluminum. The approximately equal standoff distances of the brilliant aluminum flame indicate that the ignition time is independent of particle size in the range investigated. In test *B-9*, the ignition of the aluminum appeared in flamelets similar to those observed by Cassel and Liebman. The sporadic ignition and combustion are believed to be attributable to the joint effects of the low temperature ($3050^\circ R$) and the low aluminum concentration. Apparently, this test was conducted at the limits of ignitability for the $44\text{-}\mu$ powder.

The burner tests demonstrated that aluminum ignition and combustion were primarily dependent upon flame temperature and particle concentration. Under rocket-engine conditions, the particle concentration of the aluminum powder would well exceed the minimum concentration necessary to ignite and sustain combustion of aluminum powder at low temperatures. Results also indicated that combustion of the aluminum would be achieved if only a small portion of the total hydrogen gas were injected with the powder to provide a pilot flame and the remainder were injected downstream of the aluminum-oxygen reaction zone.

Open-Flame Tests

Three open-flame tests were made to determine the injection method and chamber configuration most conducive to producing efficient combustion and mixing of the O_2 - H_2 -Al powder system in a 100-lbf-thrust rocket engine. Two basic injector designs, flat-faced and hemispherical, were initially employed. The flat-faced injector eroded in the initial tests. Cylindrical Lucite chambers having an inside diameter of 2.25 in. and a length of 4 in. were used to permit high-speed photography of the combustion process. No nozzles were employed in the open-flame test series. Ignition was accomplished by discharging 2000 v across insulated wires taped to the injector face. The O_2 - H_2 MR was approximately eight.

The open-flame tests indicated that efficient aluminum combustion occurred when a minimal portion of the hydrogen was used to deliver the aluminum, whereas the major part of the hydrogen was injected downstream from the $Al + O_2$ ignition region. As predicted from the results of the burner tests, this permitted the aluminum to burn in the high-oxygen-content region and then heat the remaining hydrogen. Photographs indicated an intense reaction at the aluminum-oxygen impingement point. The H_2 injected downstream could be seen to slightly quench the $Al + O_2$ reaction as it mixed with the combustion products.

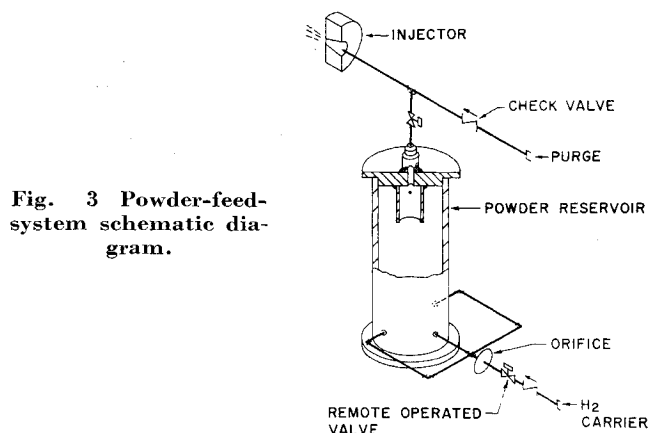


Fig. 3 Powder-feed-system schematic diagram.

Small-Scale Performance Tests

The theoretical performance of the gaseous O_2 -gaseous H_2 -aluminum propellant system was calculated using the chemical-composition computer program developed by Aerojet-General. The calculations were made for shifting equilibrium adiabatic expansion assuming complete thermal and velocity equilibrium of the condensed phase with the expanding gases. The theoretical performance is given in Fig. 4. The optimum theoretical specific impulse for O_2 (gas)- H_2 (gas) is 364.5 sec at an MR of 2.8. The addition of 50% (weight) of aluminum to the hydrogen increases the theoretical performance to 368 sec at an MR of 0.75.

Twenty tests were made in the 100-lbf-thrust engine with the hemispherical injector and the copper chambers and nozzles. Fourteen were made to determine optimum injector configuration, mixture ratio, and chamber characteristic length L^* . The hemispherical injector showed no significant erosion. The hydrogen ring was placed at the injector in the center of the combustion chamber and immediately in front of the nozzle (Fig. 2); impingement angle (included angle) was 60° (tests 1-7 and 11-20) or 120° (tests 8-10). The L^* was 120 in. for test 1, 220 in. for test 3, 270 in. for tests 12 and 13, and 170 in. for the other tests.

From tests 1-14, it was found that the hemispherical injector yielded highest performance when the hydrogen ring was placed against its face, with an impingement angle of 60° ; the best L^* was 170 in. The high performance obtained with this configuration was attributed to the high oxygen concentration at the O_2 -Al impingement zone and to the high temperature of the O_2 -Al flame, estimated to be approximately $7000^\circ R$. The large L^* provided a long residence time for the O_2 -Al reaction and heat transfer from the metal oxide to the hydrogen working gas. Tests 15-20 were conducted at optimum conditions to determine the percentage of theoretical I_{sp} obtainable. The highest I_{sp} obtained was 286.1 sec at an over-all mixture ratio of 1.18 for

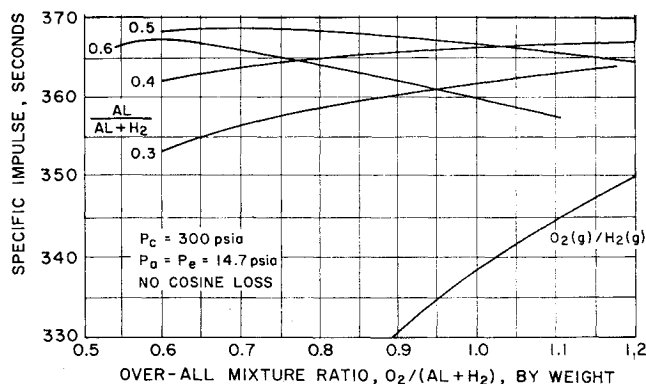


Fig. 4 Theoretical performance of O_2 (gas)- H_2 (gas)-Al.

Table 2 Performance test data

	Al Al + H ₂ , by wt.	O ₂ H ₂ + Al, by wt.	Total input \dot{m}_t , lb/sec	Al ₂ O ₃ deposition \dot{m}_d , lb/sec	P_c , psia	Q to walls, Btu/sec	Ring location ^a	Specific impulse exp., sec	% theo., I_s
1	0.46	2.13	0.339	0.040	373	...	0	277	76.3
2	0.29	2.82	0.305	...	314	...	0	291	80.1
3	0.47	2.38	0.325	...	289	...	150	247	71.6
4	0.38	1.95	0.331	...	314	...	100	269	74.1
5	0.45	0.93	0.272	...	204	...	100	201	80.4
6	0.41	2.02	0.328	...	335	...	100	275	75.5
7	0.51	1.62	0.330	0.046	243	...	100	243	67.7
8	0.48	1.99	0.339	...	338	...	100	241	67.2
9	0.48	1.97	0.358	...	312	...	50	229	64.4
10	0.45	1.45	0.324	...	315	...	0	259	71.7
11	0.48	1.64	0.310	...	290	...	50	255	71.3
12	0.38	2.16	0.287	0.008	274	...	150	259	72.8
13	0.49	1.50	0.317	0.045	303	...	0	267	74.0
14	0.49	1.88	0.301	0	310	...	0	285	80.2
15	0.41	0.61	0.240	0.007	222	160.6	0	240.3	68.8
16	0.28	0.83	0.202	0.002	200	143.1	0	253.1	76.1
17	0.42	0.83	0.244	0.002	257	157.2	0	265.3	73.9
18	0.31	1.21	0.233	0	244	198.0	0	270.2	76.0
19	0.24	1.18	0.239	0.001	258	231.0	0	286.1	80.5
20	0.28	1.19	0.233	0.001	250	205.0	0	279.9	78.7

^a Location of H₂ injection ring at L^* station; zero indicates ring at injector face.

O₂-(0.76 H₂ + 0.24 Al); this was 80.5% of the theoretical I_{sp} .

Observation of the P_c traces recorded on the oscillograph indicated smooth ignition and combustion of the aluminum. The spark igniter started the O₂-H₂ reaction, which in turn ignited the aluminum powder. No hard starts occurred. All performance tests were stable.

Performance Evaluation

A combination of experimental techniques and theoretical calculations was used to outline the major performance losses for the 100-lbf engine. The major loss resulted from heat loss to the copper thrust chamber. To determine the heat loss, thermocouples were placed in the thrust chamber to determine the heat absorbed by the chamber. The average heat-rejection rate was between 140 and 230 Btu/sec. Significant amounts of Al₂O₃ were deposited on the thrust-chamber walls in some of the firings (Table 2). The deposits, collected and weighed after each firing, reduced the mass flow through the nozzles. The combined effect of heat rejection and deposition on performance was calculated on a 1-sec basis. The derivation starts with the basic thrust equation

$$I_s = F/g\dot{m}_t = (\dot{m}_t - \dot{m}_d)V/g\dot{m}_t \quad (1)$$

where F = thrust of rocket engine, g = acceleration of gravity, V = exhaust velocity of the propellants, \dot{m}_0 = mass flow rate of propellants flowing out of the thrust chamber, \dot{m}_t = total mass flow rate of propellants flowing into the thrust chamber, and \dot{m}_d = mass deposition rate of propellants deposited in the thrust chamber. From the general energy equation, $\Delta H - Q = \frac{1}{2}\dot{m}_0 V^2$, where ΔH = enthalpy change of propellants from injector to exhaust, Q = total heat transferred to the thrust-chamber assembly, and

$$V = [2(\Delta H - Q)/\dot{m}_0]^{1/2} \quad (2)$$

Combining Eq. (2) with Eq. (1), I_s , corrected for heat transfer and deposition, is

$$I_s = (\dot{m}_t - \dot{m}_d)[2(\Delta H - Q)/\dot{m}_0]^{1/2}/g\dot{m}_t \quad (3)$$

The results of these calculations indicated that the combined effects of heat loss and deposition caused an estimated performance loss of about 10% of the theoretical specific im-

pulse for the rocket-engine tests with the optimized hydrogen ring placement.

Theoretical calculations for gas-particle flow losses were made using a one-dimensional computer program⁶ to calculate the performance loss that results from particle velocity lags and particle thermal lags. The results of these calculations are shown in Fig. 5; it is seen that the performance loss increases as particle size increases. Six tests were conducted with O₂-H₂-Al₂O₃ mixtures in the 100-lbf-thrust engine, using 5- μ average diameter Al₂O₃ particles. The weight fraction of the Al₂O₃ was varied from 5 to 33%, and the theoretical chamber temperatures were kept below the melting point of Al₂O₃ (4172°R) to prevent agglomeration of the Al₂O₃ particles. The experimental points agreed well with the theoretically predicted 5- μ curve (Fig. 5). Aluminum oxide particles were also collected from the O₂-H₂-Al firings by deposition on sheets of aluminum foil placed 15 ft from the nozzle. Examination with an electron microscope showed that the particles were 1 μ or less in diameter. Figure 5 indicates that this would lead to a loss of about 1% of the theoretical specific impulse.

The effect of the half-angle divergence factor on performance amounts to a 2% loss in performance for the micro-engine.⁷ The performance loss due to skin-friction drag was calculated for the nozzle from generalized charts⁷ prepared by the Rubesin, Maydew, and Varga⁸ extension of the Frankl-Voishel analysis. The loss from friction was about 1%.

The particles from the firings and the chamber deposits were collected and analyzed. All of the aluminum was present as aluminum oxide. From this the writers surmised that the performance loss due to combustion inefficiency should be similar to that of larger-scale rocket engines using conventional propellants, or about 4-6% of the theoretical specific impulse. However, the other performance losses considered previously add up to 14% of the theoretical specific impulse. Since the experimentally measured loss was 20%, the remaining 6% is attributed to combustion inefficiency and/or experimental error.

Effect of Rocket-Engine Size on Performances

The small size of the 100-lbf-thrust engine emphasizes performance losses caused by irreversible processes. An estimate of the performance losses to be expected from the

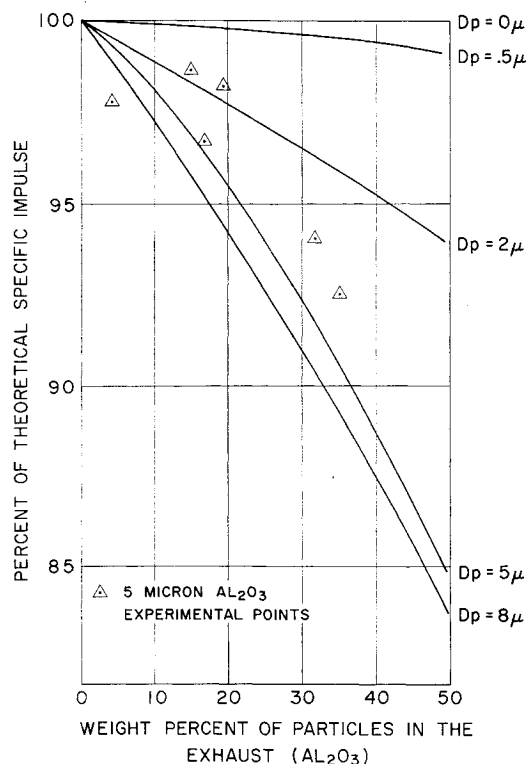


Fig. 5 One-dimensional gas-particle flow performance losses.

$\text{O}_2\text{-H}_2\text{-Al}$ propellant system in the 100-lbf microengine, an uncooled 5-K-lbf development engine with a conical nozzle and a regeneratively cooled 200-K-lbf engine with a contoured nozzle is given in Fig. 6. The propellant used gives 40% condensed phase in the exhaust. It is seen that the microengine gives 81% of theoretical specific impulse, the 5-K-lbf engine, 92%, and the 200-K-lbf engine, 93.5%. The major loss in the microengine (10%) is the result of heat transfer to the chamber; this loss is smaller (3%) for the 5-K-lbf engine and negligible for the regeneratively cooled 200-K-lbf engine as the incoming propellants are used as the cooling medium. A combustion inefficiency of 4% is assumed to be the same in all three engines. Geometry and friction losses account for about 4% of the performance degradation in the microengine, 3% in the 5-K-lbf engine, and 3% in the 200-K-lbf engine. The geometry and friction losses are similar for the 5-K-lbf engine because of 5-K-lbf engine having a conical nozzle and the 200-K-lbf engine having a contoured nozzle. Gas-particle flow losses were calculated on the basis of a $2\text{-}\mu$ average particle size of Al_2O_3 in the exhaust. With this particle size, the gas-particle flow losses are calculated to be 4% in the microengine, 2% in the 5-K-lbf engine, and 1% in the 200-K-lbf engine.

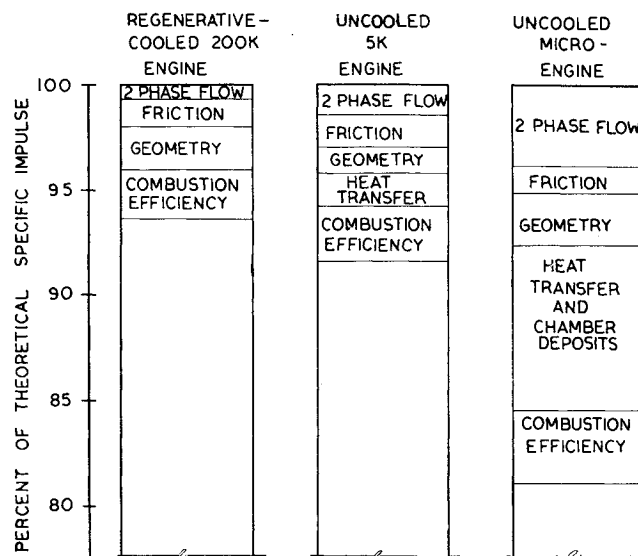


Fig. 6 Theoretical performance-loss comparison.

Conclusions

A fluidized transport system for the delivery of the Al powder was developed and used successfully. The data obtained from the 100-lbf-thrust microengine tests indicated successful firing of the $\text{O}_2\text{-H}_2\text{-Al}$ propellant system. Analysis indicated smooth ignition and combustion of the aluminum particles. Once ignited, the Al appeared to burn stably as evidenced by the negligible fluctuations in chamber pressure. The combustion efficiency was estimated to be between 94 and 96%.

References

- Hartmann, J., "Recent research on the explosibility of dust dispersions," *Ind. Eng. Chem.* **40**, 752 (1948).
- Markstein, G. H., "Combustion of metals," *AIAA J.* **1**, 550-562 (1963).
- Friedman, R. and Macek, A., "Ignition and combustion of aluminum particles in hot ambient gases," *Combust. Flame* **6**, 9-19 (March 1962).
- Gordon, D. A., "Combustion characteristics of metal particles," *ARS Progress in Astronautics and Rocketry: Solid Propellant Rocket Research*, edited by M. Summerfield (Academic Press Inc., New York, 1960), Vol. 1, pp. 271-278.
- Cassel, H. M. and Liebman, I., "The cooperative mechanism in the ignition of dust dispersions," *Combust. Flame* **3**, 467-475 (December 1959).
- Glauz, R. D., "Combined subsonic-supersonic gas-particle flow," *ARS J.* **32**, 773-775 (1962).
- "Study of high effective area ratio nozzles for spacecraft engines," Third Quarterly Progress Report, Aerojet-General Rept. 9232:7-136-03-Q (February 1, 1963).
- Rubeson, M. W., Maydew, R. C., and Varga, S. A., "An experimental and analytical investigation of the skin friction of the turbulent boundary layer on a flat plate at supersonic speeds," NACA TN 2305 (February 1951).